JOURNAL OF CATALYSIS 112, 375–383 (1988)

Characterization of Chromia-Promoted γ-Iron Oxide Catalysts and Their CO Conversion Efficiency

M. L. KUNDU,* A. C. SENGUPTA,* G. C. MAITI,* B. SEN,* S. K. GHOSH,* V. I. KUZNETSOV,† G. N. KUSTOVA,† AND E. N. YURCHENKO†

*R&D Division, Projects & Development India Limited, Sindri—828 122, Dhanbad, India, and †Institute of Catalysis, Novosibirsk 630090, USSR

Received September 29, 1987; revised February 17, 1988

A systematic study has been conducted on the evolution of phases in chromia-promoted γ-Fe_2O_3 catalysts prepared under a wide range of conditions using different instrumental techniques, viz., DTA, XRD, TEM, IR, and Mössbauer spectroscopy. The structural parameters have been correlated with the reaction properties of the catalysts for the water gas shift reaction. It has been revealed that γ-Fe_2O_3 prepared by precipitation techniques has an imperfect spinel structure. In the wet mixing method of preparation of the catalyst, the interaction between γ-Fe_2O_3 and Cr_2O_3 is found to be insignificant, while for the coprecipitated method, the interaction takes place by the incorporation of Cr^{3+} ions into the octahedral vacant sites of the γ-Fe_2O_3 lattice where chromia concentration remains below 15%, above which the crystallization of the mixed phase is hindered and the activity of the catalyst tends to decrease. The reverse coprecipitation technique with a chromia concentration of nearly 10% is found to be most effective for imparting higher CO conversion activity.

INTRODUCTION

Chromia-promoted iron oxide is widely used as a water gas shift reaction catalyst in which iron oxide mass initially exists in any of the crystalline forms, viz., α-Fe_2O_3, γ-Fe_2O_3, or hydrated iron oxide, and chromia is used as a structural promoter (*1–3*). The incorporation of Cr^{3+} ions into α-Fe_2O_3 lattice occurs readily by a continuous cationic interdiffusion process (*4, 5*). But the same is not true for γ-Fe_2O_3 which differs in structural symmetry from α-Cr_2O_3. Both α- and γ-Fe_2O_3 are reduced to Fe_3O_4 to obtain the active catalytic mass for the water gas shift reaction. Since the reduction of γ-Fe_2O_3 into Fe_3O_4 is effected by topotactic transformation (*6*), sintering of the active phase is greatly reduced in catalysts consisting of γ-Fe_2O_3 compared to that of α-Fe_2O_3 under identical operating conditions. Because of this property, γ-Fe_2O_3 is preferentially used for the commercial production of high-temperature shift catalysts (*7–11*). However, no systematic study has been reported so far for the identification of the nature of Cr^{3+} species in the catalytic system consisting of γ-Fe_2O_3/Cr_2O_3. Only limited information is available in published literature (*7, 12*).

γ-Fe_2O_3 possesses an imperfect spinel structure in which Fe^{3+} ions are distributed in tetrahedral and octahedral positions with cation vacancies preferentially located at octahedral lattice sites (*13–15*). Because of the preferential distribution of vacancies at octahedral sites, Fe^{3+} ions are more strongly bound at the tetrahedral lattice points (*13, 16*). According to Verwey (*14*) and Kordes (*15*) the structure of γ-Fe_2O_3 can be represented as $(Fe_1^{3+})_{tetr.}(\square_{1/3}Fe_{5/3}^{3+})_{Oct.}O_4$, where $\square_{1/3}$ denotes nearly 11% cation vacancies per molecule. It therefore seems possible that in the chro-

0021-9517/88 $3.00

mia-promoted γ-Fe_2O_3 catalysts, Cr^{3+} ions can be incorporated into the octahedral vacant sites of γ-Fe_2O_3.

With this goal in mind, in the present investigation, a systematic study has been carried out on the identification of the nature of incoporation of Cr^{3+} ions and the evolution of phases in chromia-promoted γ-Fe_2O_3 catalysts prepared under different conditions as well as the structural parameters and their effects on the catalytic activities for water gas shift reactions.

EXPERIMENTAL

Three series of samples were prepared for this study and will be denoted as A, B, and C. γ-Fe_2O_3 was prepared by oxygenation of iron hydroxide slurry in alkaline medium. The precipitated mass was washed to free it from SO_4^{2-} ions and calcined at 473 K for 1 h. This sample was designated A. The three samples in this series were prepared by kneading (incipient wet mixing) γ-Fe_2O_3 with chromium(VI) oxide solution to have nearly 10, 15, and 20% Cr_2O_3 by weight after calcination and were designated A1, A2, and A3, respectively. B series samples were prepared by the coprecipitation of ferrous sulfate and chromium(III) sulfate solutions (0.1 *M* each) with 0.25 *M* NaOH solution under an inert atmosphere, followed by oxygenation of the hydroxide slurry in an alkaline medium. The precipitated mass was washed to free it from sulfate ions and was oven dried at 383 K. Three samples, namely B1, B2, and B3, were prepared with nearly 10, 15, and 20% Cr_2O_3 by weight, respectively. Samples C1, C2, and C3 with about 10, 15, and 20% Cr_2O_3 by weight in the calcined product, respectively, were prepared by a reverse precipitation technique, i.e., by the addition of mixed ferrous and chromium(III) sulfate solution to sodium hydroxide solution. The other treatments were the same as those used for the B series. The difference between the B and the C series is that in the B series the metal hydroxides are precipitated one after another depending on the solubility products, whereas in the C series both hydroxides are precipitated simultaneously. Another sample designated D was prepared by mechanical mixing of γ-Fe_2O_3 with 10% Cr_2O_3. The chromia-incorporated samples were calcined for 1 h at respective temperatures as shown in Table 1. The chemical analyses for iron and chromium in all the samples were performed using standard analytical methods.

Differential thermal analysis was carried out in a DTA instrument fabricated in PDIL Workshop. The heating rate was maintained at 10 K/min, and α-Al_2O_3 was used as standard. The preheat treatment of the

TABLE 1

Crystal-Phase Composition and Structural Parameters of γ-Fe_2O_3/Cr_2O_3 System at Different Temperatures

Name of sample	% Cr as Cr_2O_3	Crystalline phases after calcination at					Lattice parameter of γ-Fe_2O_3 at 723 K (Å)	Crystallite size of γ-Fe_2O_3 at 723 K (Å)	Surface area (m^2/g)
		473 K	623 K	723 K	873 K	973 K			
A	0	γ-Fe_2O_3	γ-Fe_2O_3	γ-Fe_2O_3, α-Fe_3O_3	α-Fe_2O_3	α-Fe_2O_3	8.335(3)	630	
A1	8.4	γ-Fe_2O_3	γ-Fe_2O_3	γ-Fe_2O_3, α-Cr_2O_3	α-Fe_2O_3	α-Fe_2O_3	8.331(4)	560	25.1
A2	13.56	γ-Fe_2O_3	γ-Fe_2O_3	γ-Fe_2O_3, α-Cr_2O_3	α-Fe_2O_3	α-Fe_2O_3	8.331(4)	560	24.7
A3	18.71	γ-Fe_2O_3	γ-Fe_2O_3	γ-Fe_2O_3, α-Cr_2O_3	α-Fe_2O_3	α-Fe_2O_3	8.330(5)	560	28.0
B1	9.86	[a]	γ-Fe_2O_3	γ-Fe_2O_3	γ-Fe_2O_3, α-Fe_2O_3	α-Fe_2O_3	8.305(6)	480	87.0
B2	15.01	[a]	γ-Fe_2O_3	γ-Fe_2O_3	γ-Fe_2O_3, α-Fe_2O_3	α-Fe_2O_3	8.304(7)	280	146.4
B3	19.74	[a]	γ-Fe_2O_3	γ-Fe_2O_3	γ-Fe_2O_3, α-Fe_2O_3	α-Fe_2O_3	8.304(7)	270	176.6
C1	9.62	[a]	γ-Fe_2O_3	γ-Fe_2O_3	γ-Fe_2O_3, α-Fe_2O_3	α-Fe_2O_3	8.301(6)	300	95.0
C2	14.76	[a]	γ-Fe_2O_3	γ-Fe_2O_3	γ-Fe_2O_3, α-Fe_2O_3	α-Fe_2O_3	8.302(7)	200	121.2
C3	19.48	[a]	[a]	[a]	α-Fe_2O_3	α-Fe_2O_3	—	—	137.7

[a] Amorphous.

kneaded samples was carried out at 573 K because of the hygroscopic and corrosive nature of free chromic acid for DTA studies.

X-ray diffraction studies were carried out with a standard Guinier camera and X-ray diffractometer using Cu$K\alpha$ radiation. θ-values were corrected by comparison with α-Al_2O_3 diffraction lines. Crystalline phases were determined by the JCPDS method and lattice parameters were determined from the θ-values using a suitable computer program. The crystallite sizes were measured by a line broadening technique using the Scherrer formula.

Electron micrographs of the samples were obtained using a transmission electron microscope (JEOL-JEM-100 CX). The samples were soaked in acetone to remove entrapped air and dispersed in isopropyl alcohol by means of an ultrasonic probe.

Infrared spectra were recorded in a SPECORD JR-75 IR spectrometer and a Bruker IFS Fourier transform IR spectrometer. The sample pellets were prepared using a CsI matrix.

The Mössbauer spectra of the samples were recorded in an NF-640 spectrometer at 295 and 77 K. Analyses of the Mössbauer spectra and the decomposition into Lorentz components were performed with the aid of an E-666 computer and SK-2 curve synthesizer. Co^{57} (Pd) with an activity of some 20 mCi at room temperature was used as a source. γ quanta were registered by a proportional counter with resolution $\Delta E_{14.4\,keV} = 15\%$. All chemical shifts were measured relative to α-Fe. Sample weights were varied within 10–25 mg/cm^2 depending upon the content of Fe in mixed oxides. The samples were placed in Teflon cuvettes having a flat parallel Be window of 0.05 mm thick.

The CO conversion activities of the samples were measured in a glass reactor in the temperature range 518–573 K using a gas composition (dry) around 8% CO_2, 20% CO, 60% H_2, 4% CH_4, and steam : gas = 1.0, overall space velocities being varied in the range 10,000–30,000 h^{-1}. The volume of the catalyst taken in each case was 1 cm^3 of −10 to +12 mesh size (B.S.). All experiments were conducted under isothermal conditions far removed from equilibrium (maximum conversion 10%). The surface areas of the samples were measured by the BET method. The samples were reduced with the same gas composition at a temperature of 523 K before activity measurements. The activities per gram catalyst sample were expressed as a first-order rate equation given by Laupichler (*17*).

RESULTS AND DISCUSSION

The DTA curves of the samples are shown in Fig. 1. In the DTA curves of samples A1, A2, and A3, an endothermic peak appears at 723 K whereas this peak is absent in sample A. This is due to formation of the Cr_2O_3 phase from the interme-

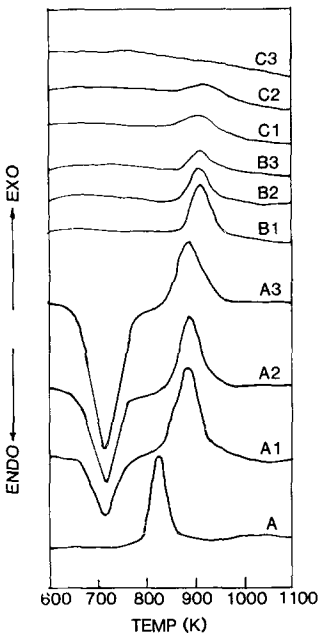

FIG. 1. DTA curves of γ-Fe_2O_3/Cr_2O_3 samples. A, γ-Fe_2O_3; A1, A2, and A3, wet mixed γ-Fe_2O_3/Cr_2O_3 having Cr_2O_3 contents of about 10, 15, and 20%, respectively; B1, B2, and B3, direct coprecipitated γ-Fe_2O_3/Cr_2O_3 having Cr_2O_3 contents of about 10, 15, and 20%, respectively; and C1, C2, and C3, γ-Fe_2O_3/Cr_2O_3 having Cr_2O_3 contents of about 10, 15, and 20%, respectively.

diate oxides of chromium, which are formed during calcination of the samples at 573 K. The intensity of the endothermic peak increases with increasing chromia concentration. This implies that free Cr_2O_3 is present in the samples of the A series and therefore, practically no interaction between γ-Fe_2O_3 and Cr_2O_3 takes place in these samples. In the case of B and C series samples, no exothermic peak around 723 K was observed in the DTA thermogram. This peak has been attributed by several workers (*18, 19*) to be due to the transformation of amorphous chromium hydroxide to crystalline chromium oxide. The absence of such a peak, therefore, indicates that in these samples, chromium hydroxide loses its identity under the present preparative conditions, thus implying the formation of a mixed hydroxide phase, which is converted into chromium-substituted γ-Fe_2O_3 upon oxidation.

The exothermic peaks, appearing in the DTA thermograms of all the samples, are accounted for by the transformation of γ-Fe_2O_3 into the α-Fe_2O_3 phase. In sample A, this peak appears at 823 K which is somewhat higher than the values reported elsewhere (*20*). In the samples of the A series, this peak is shifted to 893 K and in the samples of the B and C series, the same is further shifted to 913 K. A similar increase in the $\gamma \rightarrow \alpha$ phase transition temperature in the presence of chromia has been reported by Danielezyk and Haber (*9*). The increase in the phase transition temperature suggests that in the presence of chromia, γ-Fe_2O_3 becomes thermally stable, and the thermal stability of the coprecipitated samples is more than that of the wet mixed samples. In the case of samples C1 and C2, the exothermic peak becomes weak and broad and disappears in sample C3. This observation reveals that the incorporation of higher concentrations (more than 15%) of chromia by the reverse coprecipitation technique, as in the case of sample C3, hinders the crystallization of γ-Fe_2O_3.

X-ray investigation results are presented in Table 1. The estimated standard deviations of the lattice parameter (a_0) values are shown in parentheses. In the case of kneaded samples (A1 to A3), γ-Fe_2O_3 is the predominate phase at the early stage of calcination, and a free Cr_2O_3 phase is present in all the samples calcined at 723 K only. The formation of a single corundum-type α-Fe_2O_3 phase has been observed at 873 K. In the case of samples B1 to B3, the crystalline γ-Fe_2O_3 phase is formed at 623 K. The transformation from the γ- to the α-phase starts around 873 K and is completed at 973 K. In samples C1 to C3, γ-Fe_2O_3 crystallizes in samples C1 and C2 at 623 K whereas sample C3 is amorphous up to 723 K. The transformation from the γ- to the α-phase takes place as in samples of B series (Table 1).

Pure γ-Fe_2O_3 (sample A) starts to transform into α-Fe_2O_3 at 723 K and is completed at 873 K. In the presence of Cr^{3+} ions this transformation temperature is elevated. The elevation of temperature is greater in coprecipitated samples than in the kneaded samples, which indicates that the thermal stability of γ-Fe_2O_3 is greater in coprecipitated samples. In the case of kneaded samples the measured lattice parameter values of γ-Fe_2O_3 at 723 K show an insignificant decrease in a_0 values (Table 1) after incorporating Cr_2O_3 into γ-Fe_2O_3. The crystallite size of γ-Fe_2O_3 (Table 1) also does not change with an increase in chromia concentration. The insignificant change in a_0 values and the presence of free Cr_2O_3 reveal that there is little interaction between γ-Fe_2O_3 and Cr_2O_3 in the kneading process. In coprecipitated samples, the change in a_0 values of γ-Fe_2O_3 from that of sample A is significant (Table 1). Moreover, the crystallite sizes of γ-Fe_2O_3 are found to decrease monotonically with increasing chromium concentration (Table 1) and the X-ray diffraction lines gradually become broad and diffuse, particularly below 723 K. This is more pronounced in the C series samples; initially, at low chromia concentration, the composite oxide is crystalline

but with an increase in Cr^{3+} content a monotonic transition from a crystalline to an amorphous state occurs. The X-ray studies, therefore, reveal that in coprecipitated samples Cr^{3+} ions can enter the γ-Fe_2O_3 lattice up to a certain concentration which is below 15%; consequently a lattice distortion takes place as is evident from the lattice parameter change. Furthermore, with the increase in Cr^{3+} content, a monotonic decrease on a long-range order of the γ-Fe_2O_3 lattice seems to occur as inferred from the gradual broadening and diffuseness of the diffraction lines. However, further studies are necessary to substantiate this.

The results obtained from X-ray diffraction were further corroborated by electron microscopic studies. The electron diffraction pattern of sample A corresponds to the γ-Fe_2O_3 phase. Free Cr_2O_3 was noted in the electron diffraction patterns of samples A1 to A3 in addition to the γ-Fe_2O_3 phase. The existence of free Cr_2O_3 was also indicated in the electron micrographs by the appearance of plate-like particles over the γ-Fe_2O_3 particles. However, no free Cr_2O_3 was noted in the coprecipitated samples (B and C series). Electron diffraction patterns also indicated a distortion of γ-Fe_2O_3 structure in the case of samples B3 and C3. This suggests that an interaction between γ-Fe_2O_3 and Cr_2O_3 has taken place in coprecipitated samples. The incorporation of Cr_2O_3 in the samples prepared by kneading does not show any major influence on the particle size of the γ-Fe_2O_3 phase. However, the γ-Fe_2O_3 particle sizes in the B and C series samples have been found to decrease appreciably by increasing incorporation of Cr_2O_3. This shows that an increase in chromia concentration in the coprecipitated samples hinders the crystal growth of γ-Fe_2O_3.

Infrared spectra of the samples of A, B, and C series, shown in Fig. 2, correspond to an imperfect spinel of γ-Fe_2O_3. This conclusion is based on the remarkable splitting of absorption bands in the regions 800–500 and 500–350 cm^{-1} into several components (720, 640, 575 cm^{-1} and 440, 410 cm^{-1}, respectively). According to Preudhomme and Tarte (*21*), these bands are due to ν_1 (800–500 cm^{-1}) and ν_2 (500–350 cm^{-1}) modes of the FeO_6 vibrations. However, Ishii *et al.* (*22*) ascribed the ν_1 mode to vibrations of both octahedra and tetrahedra and ν_2 to those of octahedra. The latter interpretation seems to be more reasonable. It can be observed from Fig. 2 that for the samples of the A series, the absorption bands are not affected significantly in the region 800–500 cm^{-1}; only the absorption bands in the region 500–350 cm^{-1} are affected nominally with respect to their relative intensities and positions (shift from 440 to 450 and 410 to 415 cm^{-1}). This suggests that in the A series samples, Cr^{3+} is not incorporated into the

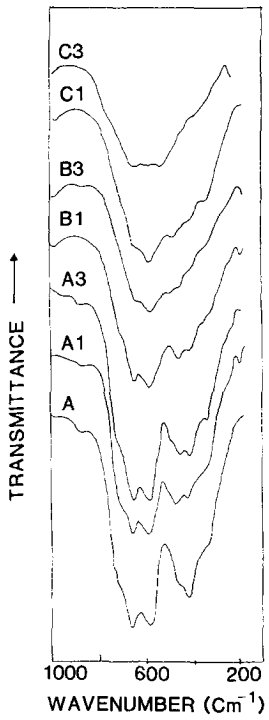

FIG. 2. Infrared spectra of γ-Fe_2O_3/Cr_2O_3 samples. A, γ-Fe_2O_3; A1 and A3, wet mixed γ-Fe_2O_3/Cr_2O_3 having Cr_2O_3 contents of about 10 and 20%, respectively; B1 and B3, direct coprecipitated γ-Fe_2O_3/Cr_2O_3 having Cr_2O_3 contents of about 10 and 20%, respectively; and C1 and C3, reverse coprecipitated γ-Fe_2O_3/Cr_2O_3 having Cr_2O_3 contents of about 10 and 20%, respectively.

TABLE 2

Value of NGR Parameters of Mixed Fe–Cr Oxides, Calcined at 673 K

Name of sample	Temperature (K)	Chem. shift δ (mm/s)	Quard. splitting Δ (mm/s)	Width of line $G_{1,6}$ (mm/s)	H_{eff} (K · Oe)	δ^a (mm/s)	Δ^a (mm/s)	$G_{1,2}{}^a$ (mm/s)
A	295	0.29	0.01	0.70 0.61	494			
	80	0.43	0.01	0.78 0.70	521			
A1	295	0.29	0.02	0.70 0.61	494			
	80	0.38	0.01	0.78 0.70	521			
A2	295	0.28	0.03	0.70 0.62	491			
	80	0.36	0	0.78 0.70	518.7			
A3	295	0.28	0.01	0.78 0.70	490			
	80	0.44	0	0.78 0.72	518.7			
B1	295	0.28	0.04	0.78 0.78	494	0.35	0.70	
	80	0.39	0	0.87 0.78	521	0.39	0.79	
B2	295	0.27	0.08	0.96 0.79	486	0.35	0.70	0.78
	80	0.42	0.02	1.05 0.79	518.7	0.39	0.79	
B3	295	0.24	0.08	0.88 0.88	488.7	0.35	0.70	
	80	0.42	0.02	0.78 0.78	515.9	0.48	0.79	
C1	295	0.30	0	0.70 0.78	488.7	0.31	0.61	
	80	0.37	0.02	0.78 0.78	518.7	0.39	0.88	
C2	295	0.24	0.06	1.05 0.46	486	0.31	0.61	
	80	0.37	0.06	1.05 0.88	510	0.44	0.88	
C3	295	—	—	—	—	0.31	0.61	0.79
	80	—	—	—	490	0.48	0.79	0.96
D	295	0.29	0.01	0.70 0.62	494	—	—	—
	80	0.40	0.01	0.78 0.62	524	—	—	—

[a] For superparamagnetic doublet.

γ-Fe_2O_3 lattice, rather it is present as a free Cr_2O_3 on the surface. For the B and C series samples, the absorption bands are significantly affected in both regions (Fig. 2); ν_2 bands are perturbed more than ν_1 bands. The absorption bands at 440 and 410 cm^{-1}

as well as 640 and 575 cm^{-1} are gradually diminished in intensity and broadened appreciably with an increase in the Cr^{3+} concentration. Also, the absorption band at 720 cm^{-1} disappears. These observations are more pronounced for samples of the C series than for those of the B series. In view of the perturbation of the absorption bands in both regions, it is evident that Cr^{3+} ions are incorporated into the γ-Fe_2O_3 lattice and a lattice distortion has also taken place. Considering the structure of γ-Fe_2O_3, it is suggested that in the case of coprecipitated samples, Cr^{3+} ions occupy mostly the octahedral vacant sites of the γ-Fe_2O_3 lattice. It is also revealed that after filling up of the vacant sites, the γ-Fe_2O_3 lattice tends to be distorted further by the inclusion of more Cr^{3+} ions as observed from the maximum broadening of the IR bands of sample C3.

Parameters of the Mössbauer spectra from samples of the A, B, C, and D series are shown in Table 2. The representative spectra are shown in Fig. 3. The spectrum of pure γ-Fe_2O_3 (sample A) has a sextet of lines ascribed to iron oxide which is close to the imperfect spinel of γ-Fe_2O_3. A distinct feature of these modifications of Fe(III) is a small value of quadrupole splitting. However, the value of δ is somewhat lower in than that of γ-Fe_2O_3 and Fe_3O_4, and H_{eff} varies over wider ranges with temperature (*23*), which can be accounted for by the imperfection of the γ-Fe_2O_3 lattice. Some asymmetry in the first and sixth most intense components of the γ-Fe_2O_3 may be due to the formation of α-Fe_2O_3 in traces. In samples of series A, the presence of Cr^{3+} ions has little effect on Mössbauer spectral parameters which remain essentially the same as those in imperfect γ-Fe_2O_3. In the Mössbauer spectra of the B series samples, a doublet appears along with the sextet from the imperfect γ-Fe_2O_3 (or spinel). This doublet can be interpreted as a superparamagnetic doublet as a result of the incorporation of Cr^{3+} ions into octahedral vacancies of the spinel. In this case, part of spin density of Fe^{3+} ions is not available for exchange. The monotonic decrease in the γ-Fe_2O_3 particle size (Table 1) with increasing Cr^{3+} concentration and the decrease in the relative spectral area of this doublet at low temperatures are consistent with superparamagnetic relaxation (*24*). Thus the appearance of doublet (Fig. 3, spectrum B2) is an indication of the interaction between Fe^{3+} and Cr^{3+} in the spinel lattice. The presence of line broadening also supports this fact, since line broadening increases with the increasing concentration of Cr^{3+} to 15% in the sample and then decreases somewhat (Table 2). The same features are characteristic for samples of the C series as well, but in this case the doublet is more intense, and line broadening is even more pronounced. This observation indicates the greater extent of the interaction between Fe^{3+} and Cr^{3+} ions in the spinel lattice. In view of the fact that parameters of the sextet remain unchanged within experimental error (±0.03 mm/s), one may conclude that except for the filling of cation vacancies in the spinel, no other mechanisms of interaction between Cr and Fe in mixed ox-

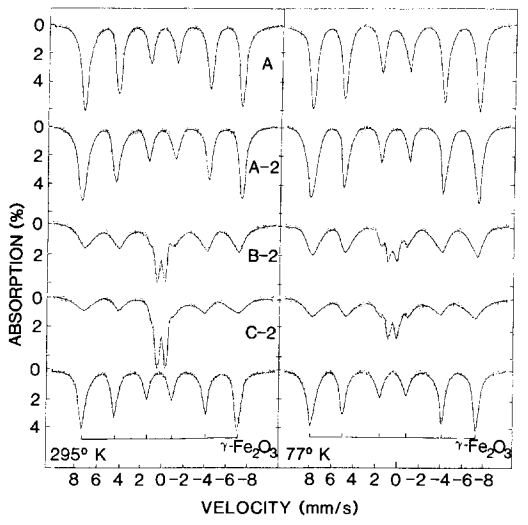

FIG. 3. Mössbauer spectra of γ-Fe_2O_3/Cr_2O_3 samples. A, γ-Fe_2O_3; A2, wet mixed γ-Fe_2O_3/Cr_2O_3 having a Cr_2O_3 content of about 15%; B2, direct coprecipitated γ-Fe_2O_3/Cr_2O_3 having a Cr_2O_3 content of about 15%; and C2, reverse coprecipitated γ-Fe_2O_3/Cr_2O_3 having a Cr_2O_3 content of about 15%.

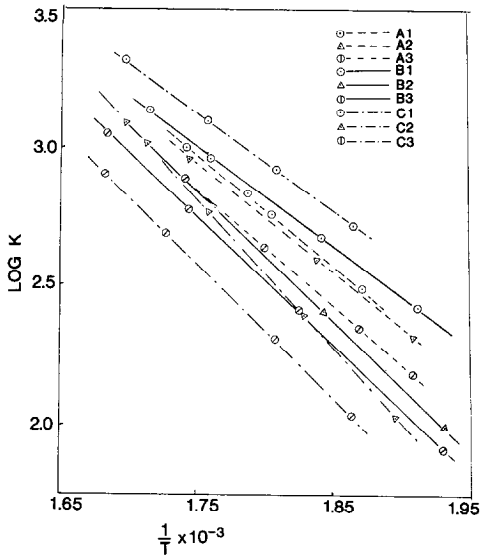

FIG. 4. Arrhenius plot of γ-Fe_2O_3/Cr_2O_3 samples. A1, A2, and A3, wet mixed γ-Fe_2O_3/Cr_2O_3 having Cr_2O_3 contents of about 10, 15, and 20%, respectively; B1, B2, and B3, direct coprecipitated γ-Fe_2O_3/Cr_2O_3 having Cr_2O_3 contents of about 10, 15, and 20%, respectively; and C1, C2, and C3, reverse coprecipitated γ-Fe_2O_3/Cr_2O_3 having Cr_2O_3 contents of about 10, 15, and 20%, respectively.

ides are realized, and excess Cr is present in the form of free α-Cr_2O_3. In sample C3 the sextet is not observed and all iron is in a superparamagnetic state.

The relative CO conversion activities of A, B, and C series sample are presented in Fig. 4. The measured apparent activation energies for all samples lie in the range 18–23 kcal · mol^{-1}. Figure 4 indicates that samples A1, B1, and C1 containing nearly 10% Cr_2O_3 have better CO conversion activities than others. Of these three samples, sample C1, in which the cationic interaction is most prominent, shows the highest CO conversion activity. However, the surface area values (Table 1) of samples B2, B3, C2, and C3 are comparatively higher than those of samples A1, B1, and C1, indicating an increase in surface area with increasing chromia content in the composite oxide. This shows that the surface area has no direct relationship with the CO conversion activity, which has also been reported by others (*25, 26*) for commercial catalysts containing γ-Fe_2O_3 and Cr_2O_3. A decrease in the activity with increasing chromia content has been observed in all series of samples. This occurs mainly due to the presence of free chromia which seems to cover the iron oxide surface. This is more prominent in the case of samples B2, B3, C2, and C3. The lattice disruption in the case of sample C3 is also an important factor for reducing its catalytic activity to the lowest value.

The studies of conversion activities reveal that the incorporation of about 10% Cr_2O_3 by weight is sufficient for preparing an effective chromia-promoted iron oxide catalyst. A similar dependence of catalytic activity on the optimum concentration of Cr_2O_3 in the case of α-Fe_2O_3/Cr_2O_3 catalyst has been reported by Markina *et al.* (*2*) and Sen *et al.* (*27*). The results also indicate that a favorable cationic interaction seems to be necessary for enhancing the catalytic activity of chromia-promoted γ-Fe_2O_3 catalyst for the water gas shift reaction. The catalytic activity remains stable until the filling up of the octahedral vacant sites of γ-Fe_2O_3 lattice by Cr^{3+} ions. However, the presence of excess chromia causes a deterioration in catalytic activity.

SUMMARY

The incorporation of Cr^{3+} ions in the γ-Fe_2O_3 lattice increases the thermal stability of γ-Fe_2O_3 as is evident from DTA and XRD studies.

In a wet mixed method of preparation of catalysts, Cr_2O_3 has little interaction with γ-Fe_2O_3 and exists as a separate phase on the surface as revealed by the different studies.

γ-Fe_2O_3 is a defect spinel having nearly 11% cation vacancies per molecule at octahedral sites. The present investigation suggests that in the case of coprecipitated samples less than 15% Cr^{3+} ions are incorporated into these octahedral vacancies. The inclusion of more than 15% Cr^{3+} ions

hinders the crystallization of the mixed phase.

The catalytic activities of the coprecipitated samples having a chromia content less than 15% are found to be greater than those of the kneaded samples. With an increase in chromia concentration, catalytic activity decreases. The surface area has no direct relationship with the conversion activity. The catalyst sample prepared by a reverse coprecipitation technique having a chromia concentration of nearly 10% shows maximum catalytic activity.

ACKNOWLEDGMENTS

The authors express their sincere thanks to Professor L. M. Plyasova, Dr. S. V. Ketchik, and Dr. E. A. Paukhstis of the Institute of Catalysis for their cooperation and valuable discussions. Thanks are also due to Mr. K. C. Banerji, General Manager (R&D), Projects & Development India Limited, for his encouragement.

REFERENCES

1. Mars, P., *Chem. Eng. Sci.* **14,** 375 (1961).
2. Markina, M. I., Boreskov, G. K., Ivanovskii, F. P., and Lyudkovskaya, B. G., *Kinet. Katal.* **2,** 867 (1961).
3. Maiti, G. C., Kundu, M. L., Ghosh, S. K., and Banerjee, B. K., *Proc. Natl. Acad. Sci. (India)* **41,** 496 (1975).
4. Dicerbo, R. K., and Seybolt, A. K., *J. Amer. Ceram. Soc.* **42,** 430 (1959).
5. Maiti, G. C., and Ghosh, S. K., *Indian J. Chem.* **24,** 513 (1985).
6. Gazzarini, F., and Lanzavecchia, G., "Proc. 6th International Symposium on the Reactivity of Solids," p. 57. Wiley–Interscience, New York, 1968.
7. Iovita, V. N., Serban, S., Iovita, C., Popa, A., and Franchy, R., *Rev. Chim. (Bucharest)* **23,** 745 (1973).
8. Badishoe Anilin, und Soda–Fabrik, A.G., Fr. 1, 566, 83109, May, 1969.
9. Danielezyk, N., and Haber, J., *Rocz. Chem.* **49**(11), 1897 (1975).
10. Maiti, G. C., Kundu, M. L., Sen Gupta, A. C., Sen, B., and Ghosh, S. K., "Proc. 2nd Indo-Soviet Seminar in Catalysis and Catalytic Reaction Engineering, R.R.L., Hyderabad, India, Nov. 25–28, 1986."
11. Sen Gupta, A. C., Kundu, M. L., Maiti, G. C., Chakraborty, B. K., Sen, B., and Ghosh, S. K., "3rd National Workshop on Catalysis and Catalysts in Chemical Industries, R.R.L., Bhubaneswar, India, Feb. 10–12, 1986."
12. Deboer, F. E., and Selwood, P. W., *J. Amer. Chem. Soc.* **76,** 3365 (1954).
13. Ferguson, G. A., Jr., and Hass, M., *Phys. Rev.* **112**(4), 1130 (1958).
14. Verwey, E. J. W., *Z. Kristallogr.* **91,** 65 (1935).
15. Kordes, E., *Z. Kristallogr.* **92,** 139 (1935).
16. Verwey, E. J. W., and Heilmann, L. L. E. L., *J. Chem. Phys.* **15,** 174 (1948).
17. Laupichler, F. G., *Ind. Eng. Chem.* **30,** 578 (1938).
18. Bhattacharya, S. K., Ramachandran, V. S., and Ghosh, J. C., "Advances in Catalysis" (D. D. Eley, W. G. Frankenburg, V. I. Komarewsky, and P. B. Weisz, Eds.), Vol. 9, p. 114. Academic Press, New York, 1957.
19. Carruthers, J. D., Sing, K. S. W., and Fernerty, J., "Proc. 6th International Symposium on the Reactivity of Solids," p. 127. 1968.
20. Mackenzie, R. C., "Differential Thermal Analysis," Vol. I, p. 276. 1970.
21. Preudhomme, J., and Tarte, P., *Spectrochim. Acta A* **27,** 1817 (1971).
22. Ishii, M., Nakahira, M., and Yamanaka, T., *Solid State Commun.* **11**(1), 209 (1972).
23. Danon, N., "Chemical Applications of Mössbauer Spectroscopy" (V. I. Goldanskii, Ed.), pp. 171–178. Moscow, 1970. [In Russian]
24. Bean, C. P., and Livingston, J. D., *J. Appl. Phys.* **30,** 1208 (1959).
25. Sen, S. P., and Sen, B., *Technology* **5**(1), 3 (1968).
26. Jovanovic, Z., and Stefanovic, M., *Hem. Ind.* **6,** 231 (1973).
27. Sen, S. P., Arora, B. R., and Ganguli, N. C., *Technology* **4,** 53 (1967).